Understanding heavy mineral separation duties using finite element analysis

by R.A. Pax*

Synopsis

Heavy mineral deposits are becoming more complex in terms of their compositional variation, particle mineralogy and size distributions, and present challenges for the operation of separation equipment to achieve the required grades and recoveries. Changes in equipment design and concepts potentially provide new opportunities for the beneficiation of heavy mineral sands deposits. The development of a framework for the fundamental understanding of separator performance issues is a first step to develop new machines. This paper will present a first step analysis of electrostatic and magnetic separation machines with their application to real separation scenarios.

Introduction

The genesis of a significant number of commercial mineral sands deposits has been the fracturing and erosion of rock from igneous intrusions followed by naturally occurring abrasion and attritioning processes that occur in stream systems, and finally in the confluence of these streams with the ocean. The naturally occurring gravity separation processes occurring in these environments have resulted in commercial heavy mineral deposits that have been traditionally characterized by a size distribution that has a mean in the vicinity of 160–200 μm with a top size in the vicinity of 250–400 μm. In the hydrological environment in which these deposits find themselves, the weathering processes, occurring over geological time frames, have resulted in modified mineral sand grains. These modifications result in some porous grains as well as surface modification of others. A more complete description can be found in Farrell *et al.* 2001 and references in it. The resultant liberated minerals can be readily beneficiated using a combination of physical separation techniques to produce a suite of products. These separation techniques include spiral, electrostatic and magnetic separators.

Mineral sands deposits that are now receiving commercial attention, contain mineral grains of slightly different physical characteristics and size distributions than previously exploited. Size distributions can have significant amounts of smaller grains. Liberation of valuable mineral can also be quite poor and particles can deviate significantly from the ideal spherical shape. These newer mineral suites sometimes present a challenge for the range of equipment that has been typically used for separation.

Consequently, pressure is bought to bear on equipment manufacturers to produce machines that are more appropriate for the particle characteristics being processed now. There is also a requirement for environmental sustainability including lower water consumption and energy use. To meet these requirements it is important to develop a greater understanding of the separation physics as well as the separator performance limitations to enable new technology to be developed. With this in mind, a fundamental science based understanding of electrostatic and magnetic separators using mathematical models is being developed.

Naturally occurring mineral sand grains such as zircon, ilmenite and rutile have ranges of values for their physical properties, which can sometimes cause misreporting of some grains to incorrect product streams. The process designer (on behalf of the operator) is faced with the challenge of identifying the correct combination of separators to produce products of sufficient grade and recovery to meet the financial requirements of a project and provide a return on invested capital.

Appropriate choice from available separator technology is required, and is a driver to develop new innovations. Although experimental approaches have traditionally been used for the innovation process, mathematical modelling based on fundamental

* *Mineral Technologies, Queensland, Australia.*

physics is also a valuable and cost-effective tool to use to solve these problems especially with the power of modern computing, software tools and well-established theories of physical and chemical phenomena. Experimental work is still required for the validation of the developed models.

Electrostatic and magnetic phenomena are the basis of key separators used in the disassembly of minerals suites found in mineral sands deposits to produce high grade mineral products. The performance of these machines can determine whether ore deposits are commercially viable or not. Although extensive modelling work of magnetic and electrostatic separators has been undertaken over the years, most of the effort has concentrated on empirical characterization of the metallurgical performance of the separators.

A common empirical approach consists of the characterization of the mineral particles independent of separator geometry and mechanics. These two modelling components are then combined using a phenomenological interaction between the two components of the approach and calibrated using experimental data. Although empirical characterization is quite useful for the development of plant designs it limits the potential opportunities to optimize existing, and/or develop new, machines.

This paper reports on some of the results of fundamental modelling of both magnetic and electrostatic separators using finite element method (FEM) techniques (see for example Cheung, 1979) and the appropriate interpretation of the results to predict metallurgical performance. The fundamental magnetic and electrostatic physics is available in a number of books; one that may be useful to the reader is written by Frankl in 1986.

Magnetic separation

To enable the separation of mineral particles using magnetic fields, particles need to have different magnetic properties, usually described as the magnetic susceptibility (χ). It is often assumed that the magnetic susceptibility, which is defined via the magnetization (***M***) response of a material as a function of an applied magnetic field (***B***) is linearly related to the applied magnetic field as shown in Equation [1]. The bold symbols are vector quantities, i.e. they have both direction and magnitude. If the susceptibility is not a function of the applied magnetic field then the material is truly paramagnetic. However, most materials of commercial interest do not exhibit paramagnetic behaviour and consequently the assumptions often made for separator design can be flawed at the outset.

$$\mathbf{M} = \chi(B)\mathbf{B} \qquad [1]$$

From Equation [1] it can be seen that the magnetization of a particle, due to the alignment of the internal atomistic magnetic moments with the applied magnetic field, is directly controlled by the applied magnetic field. When the individual magnetic moments are all aligned then the material has been magnetically saturated and any further application of an increasing magnetic field will not increase the magnetization of the particle and Equation [1] no longer applies.

A nonlinear characteristic for the magnetization behaviour usually indicates that there is some interaction between magnetic moments within the material, so that a relatively small magnetic field causes a significant amount of alignment of the magnetic moments. In the extreme case of a very strong interaction (e.g. a ferromagnet) a small applied magnetic field can magnetically saturate the particles at quite small magnetic fields.

In a magnetic separator, the magnetization of the sample then interacts with the magnetic field gradient to physically move the particle under the action of a magnetic force. The magnetic force (***F***) on a particle is described by Equation [2], where ∇ is the gradient operator.

$$\mathbf{F} = (\mathbf{M}.\nabla)\mathbf{B} \qquad [2]$$

From Equation [2], it is clear that an object has to be magnetized before a field gradient can move it. It is also clear that if the magnetization or the magnetic field gradient is large then the particles will move easily. If both values are large then the particle will move very easily. For a magnetic separator to be useful, the generated magnetic field has to magnetize the valuable more than the gangue particles and has to be inhomogeneous so that the more magnetized particles can be physically moved away from the gangue material.

Since the acceleration on a particle for a given force is inversely proportional to its mass, smaller particles are moved more easily than larger particles of the same composition, thus naturally introducing a size dependence into magnetic separation. However, the magnetic force competes with other forces that may be present such as gravitational, fluid drag and interparticle collision forces. It is the dominance of the magnetic force out of all these forces that allows the magnetic separation of a mixture of particles.

An assumption often made in the design of magnetic separators is that the magnetization is aligned with the magnetic field, which acts only radially and is reducing away from the field source. If the particles are also truly paramagnetic the magnetic force acts in the radial direction and has a magnitude as shown in Equation [3]. This is an approximation to an actual separator and naturally occurring minerals.

$$F = -\chi \frac{1}{2}\frac{dB^2}{dr} \qquad [3]$$

An additional complication for magnetic separator design is that naturally occurring minerals have a range of properties because of impurities, as well as their thermal and mechanical history. Consequently, the practical performance of a magnetic separator will not be ideal, no matter how well it is designed.

From the preceding discussion, it is clear that irrespective of the value of the magnetization of a particle, if no field gradient exists then no separation will occur, no matter what the value of the applied field. Unlike a large number of general magnetic applications, the minerals industry requires separators with very significant magnetic field gradients.

The core design question then becomes how to generate significant magnetic field gradients, with appropriate magnetic field strengths, in a volume comparable to the size of the particles, at reasonable cost compared to the added value that the separator achieves in its mineral separation duty.

Ancillary questions, such as how to present the feed material to make sure every particle is presented to the separation fields the same way are also very important but will not be discussed in this paper.

A primary tool for the evaluation and design of magnetic fields is the finite element methodology (FEM). With the FEM approach, likely magnet geometries are configured and a large number of calculation elements (points) are established. The underlying equations that describe the magnetic field patterns are then used to iteratively provide a self-consistent calculated result within the constraints of the known physics and design boundaries.

The underlying physical equations were established a long time ago and have been experimentally verified on numerous occasions in a diverse range of applications. However, their implementation in the FEM software and the material values need to be experimentally verified before confidence can be established in the solutions generated. The mathematical stability of the solution also needs to be determined, since it influences the errors of the calculation.

FEM calculations can provide information at point locations within the defined design boundaries. Practical mineral particles, however, have a finite volume and so the magnetic field and the particles magnetization will vary throughout that particle volume. The total magnetic force acting on a particle will thus be particle shape and size dependent. In contrast the gravitational force acting on a whole particle is independent of the distribution of the mass.

Magnetic separation: results and discussion

There are three types of magnetic separator types that will be discussed in the subsequent paragraphs, which are indicative of the range of magnetic separators that are used in mineral sands operations. In all cases the calculated magnetic field and field gradients can be used together with particle properties to determine the forces acting on a particle.

Rare earth roll separator

The first magnetic separator to be considered is the rare earth roll (RER) which is commonly 100 mm or so in diameter. The RER consists of rare earth magnetic plates that are magnetized along the rotational axis direction of the RER. These are sandwiched in between thinner plates of magnetizable steel. A design parameter is the thickness of the steel plate compared to the thickness of the magnetized plate; its variation results in different field gradients and field strengths. The metallurgical formulation of the rare earth magnets also influences the magnetic field properties but is not part of this paper.

Figure 1 shows the magnetic flux density pattern of an RER roll with 4 mm discs of rare earth magnet and 1 mm discs of steel plate. For dimensional guidance, 0.2 mm spaced lines are drawn above the roll. Typically, these rolls are used with non-magnetic belts that are of thickness 0.15 mm and 0.6 mm for mineral transportation.

Of interest in Figure 1 is the close to zero magnetic flux density in the bulk of the steel plates. The magnetic flux density is encoded with the colours on the scale shown to the right of the figure. Consequently, colour differences over a distance represent the magnetic field gradients that are responsible for the forces on the particles. Significant field gradients exist only within approximately 0.25 mm of the roll surface. The largest magnetic field differences occur nearest the joins of the magnetic discs and the steel plates. Beyond 0.3 mm away from the roll, only small magnetic field gradients exist and so it would be expected that this region would not contribute as significantly to separation performance of an RER, as is known.

Figure 2 shows the finite element calculations for a 4 mm rare earth magnet together with a 2 mm steel plate sandwich. In this case, there is a more pronounced (approximately zero) field region on the roll surface in the centre of the steel plate. The largest magnetic field gradient is still located within 0.25 mm of the roll surface, but more area is available for the deposition of 0.16 mm particles on the roll surface. This result is also consistent with current metallurgical observations. From the data of Figures 1 and 2, it would seem that a 0.6 mm belt around a RER roll is of limited value.

For both RER rolls, the magnetic field strength at 1.5 mm away from the roll surface is quite small, as is the magnetic field gradient, so the RERs would not capture particles flying about in this region. Feed presentation, so that particles do not bounce around, is therefore essential for metallurgically efficient operation.

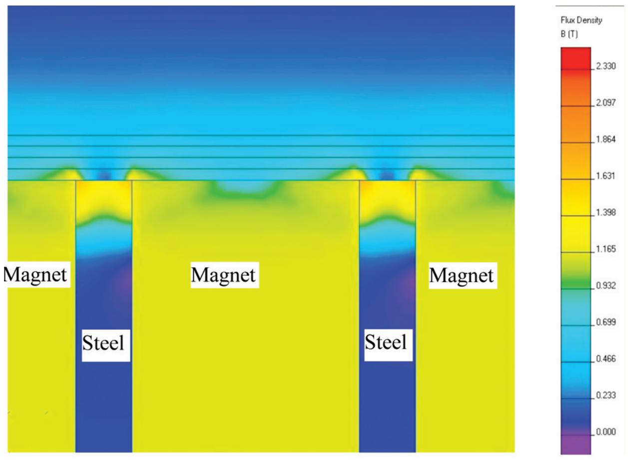

Figure 1—Finite element calculation of the magnetic field pattern of a 1 mm steel / 4 mm rare earth magnet sandwich array of a rare earth roll (RER). The horizontal lines above the roll are 0.2 mm apart

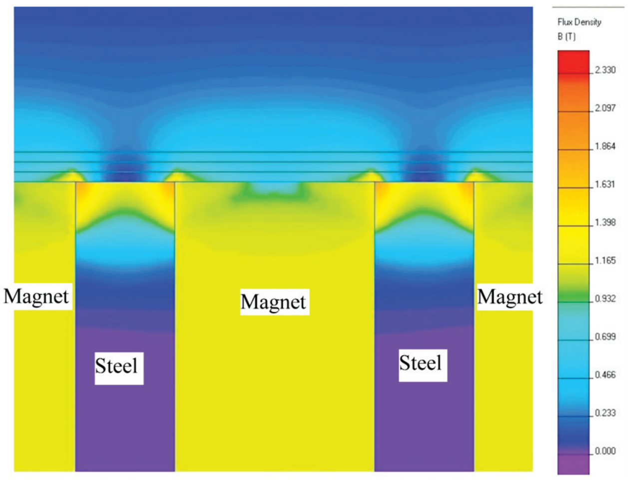

Figure 2—Finite element calculation of the magnetic field pattern of a 2 mm steel / 4 mm rare earth magnet sandwich array of a rare earth roll (RER). The horizontal lines above the roll are 0.2 mm apart

Understanding heavy mineral separation duties using finite element analysis

Rare earth drum separator

Typically rare earth drum separators are of a significantly larger diameter than the RER, which then allows a stationary rare earth magnet array to be used as shown in Figure 3. This type of magnet array essentially consists of successive magnetic circuits. The magnetization of the individual rare earth magnet segments are appropriately orientated to result in the magnetic field lines as shown in Figure 3. The maximum magnetic field strength within the array can be very high. A rotating drum is required to transport the mineral around the magnetic array at a small distance away from the array, so the magnetic field strength that the mineral particles experience will be reduced.

The magnitude of the magnetic flux density over the face of the magnetic array is reasonably uniform with fluctuations of approximately 4% of the mean field as shown in Figure 4. However, there are two fluctuating components, one normal to the surface of the drum and the other tangential to the surface of the drum (in the rotational direction). The tangential component of the magnetic field parallel to the axis of rotation of the drum is very small unless the magnetic array is poorly constructed. This tangential component does become non-zero at the ends of a drum. Figure 4 also shows the magnetic field reducing to zero in a controlled way using the trailing poles located 110 degrees from the top of the drum.

As before, the colour differences in Figure 3 are indicative of the magnetic field gradients available to move particles on the surface of the drum. It is clear from Figure 3, that the combination of field and field gradient has a limited penetration beyond the drum surface. This is more clearly shown in Figure 5.

In Figure 5 the magnetic field normal to the drum surface is denoted as B_n whilst the tangential component is shown as B_t. Their respective field gradients are shown as dB_n/d_R and dB_t/dR. For a paramagnetic material, it is the product of magnetic field and field gradient that determines the distance from the drum surface that is useful for magnetic separation.

In both cases shown in Figure 5 the product, which is related to the force, is negative, indicating an attraction of magnetic mineral to the drum surface. The magnetic force, however, is less for position 2 indicated in Figure 3. For this RED, the product is very small after about 40–50 mm from the drum surface. In practice, it turns out, that the useful distance from the drum surface for this type of RED is more like 10 to 20 mm for a dry application and 5 to 10 mm for a wet magnetic separation application, depending on what separation efficiency and duty is tolerable.

So far the discussion has assumed that the particle sizes are small compared to the magnetic field and magnetic field gradient homogeneity volume of a particular design. This assumption is reasonably valid when the particles are up to 150 mm diameter. Increased complexity occurs with particle sizes that a significantly greater than 150 mm.

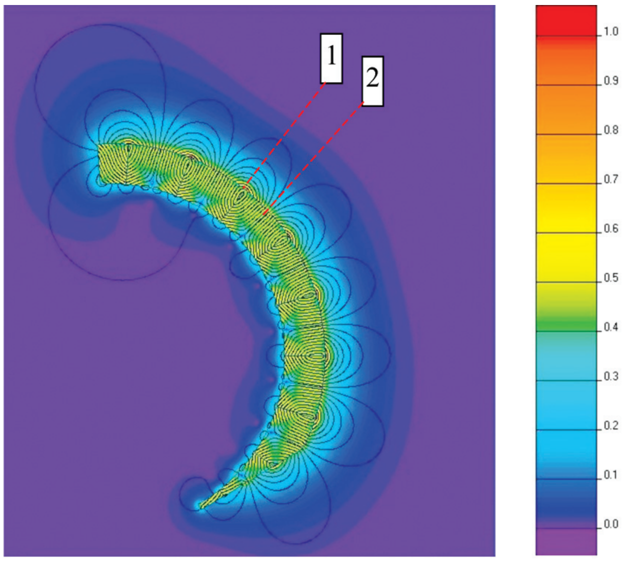

Figure 3—Magnetic flux density due to an rare earth magnet array used inside a drum. The magnetic field lines are also shown. Two contour lines are shown at positions 1 and 2. The normalized scale for the flux density is shown on the right

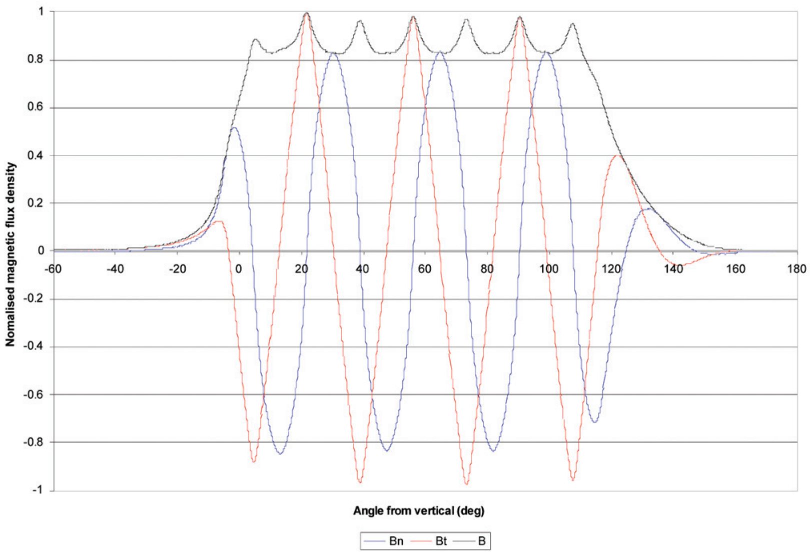

Figure 4—The total (*B*), normal (*B_n*) and tangential (*B_t*) components of the normalized magnetic flux density along a contour 1 mm above the drum surface

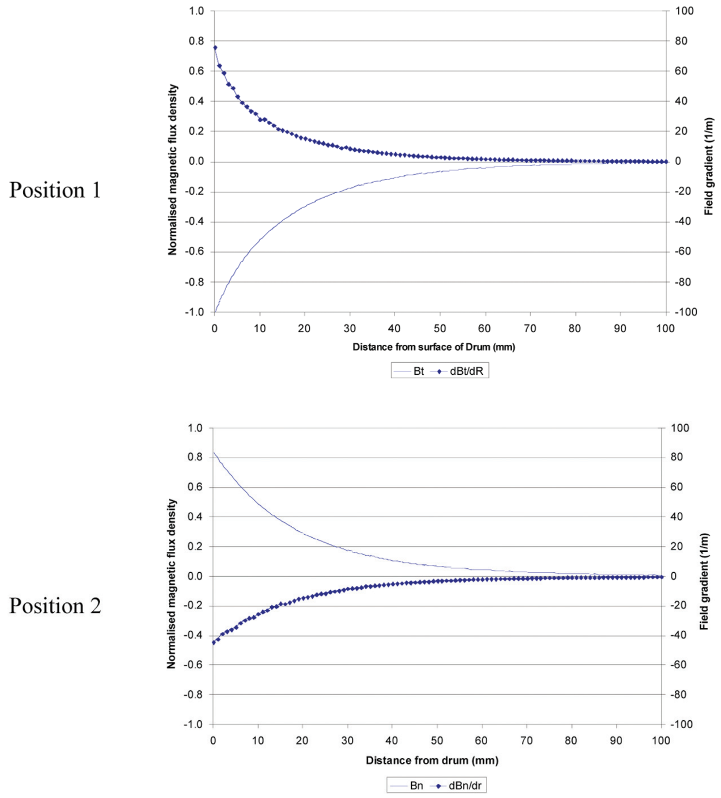

Figure 5—Normalized magnetic field (B_n and B_t) and field gradient (dB_t/dr and dB_n/d_r) for the two extreme locations of particles on a RED, see Figure 3

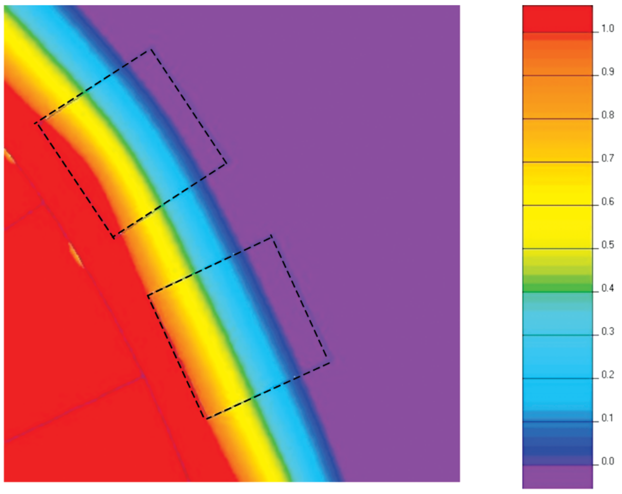

Figure 6—Slight distortion of the magnetic field pattern within 30 mm cubic 'rocks' (shown as dotted lines) located on a 400 mm diameter drum. A normalized magnetic flux density scale is given on the right

Figure 6 shows the effect on the magnetic field patterns of a rare earth drum of a 30 mm 'cubic' rock. Very little perturbation of the magnetic field pattern is evident; however, the magnetic field and field gradient are not uniform throughout the rock volume. Consequently the magnetization of the rock elements vary with their location, resulting in a force distribution throughout the rock. The applicability of this scenario is shown in Figure 7.

Figure 7—Photo of rocks leaving a drum. Approximate rotational speed was 4 rpm

Understanding heavy mineral separation duties using finite element analysis

Using the same finite element model as that used for Figure 3, rocks of different sizes were used to calculate the magnetic force on the rocks and compared to the gravitational force on the same rock. The gravitational force will always act on the whole rock. The results of this calculation are shown in Figure 7. Both a high susceptibility ore and a low susceptibility ore have been used for comparative purposes.

As expected for large rocks, the ratio of the magnetic force to the gravitational force decreases significantly as the size of the rock increases. For the low susceptibility ore a particle size of approximately 10–15 mm is sufficient for the force ratio to be equal to unity. For the higher susceptible ores the ratio is a mere 3 with 40 mm cubic rocks. These values compare to ratios in excess of 40 when the particles are 150 mm diameter.

Although it is unlikely that particle sizes greater than a 1 mm or so are to be processed using a RED in a mineral sands application, the above calculations illustrate that indeed magnetic separation is particle size dependent because of the significant field gradients that exist with rare earth drum magnetic array.

Wet high intensity magnetic separator

The last magnetic application that will be discussed is the wet high intensity magnetic separator (WHIMS) used to beneficiate low to medium susceptibility ores from non-magnetic gangue. Again a dual (electromagnet) magnetic circuit is used, as shown in Figure 9. A mild steel yoke is incorporated together with an array of salient plates with a well defined gap between them. The array of salient plates is commonly called the ‘matrix’ and is shown in the top of Figure 9. The electromagnetic coils provide sufficient energizing current to generate a large magnetic flux density in the gaps between the salient plates. The salient plates are of such geometry so that high magnetic field gradients are produced in the spaces where the mineral slurry flows, which is into the page of Figure 9. The large magnetic fields can produce sufficient magnetization in ‘magnetic’ particles so that the field gradient can provide sufficient force to encourage the magnetic particles to adhere to the salient plates in spite of erosion, gravitational and fluid dynamic forces trying to dislodge them.

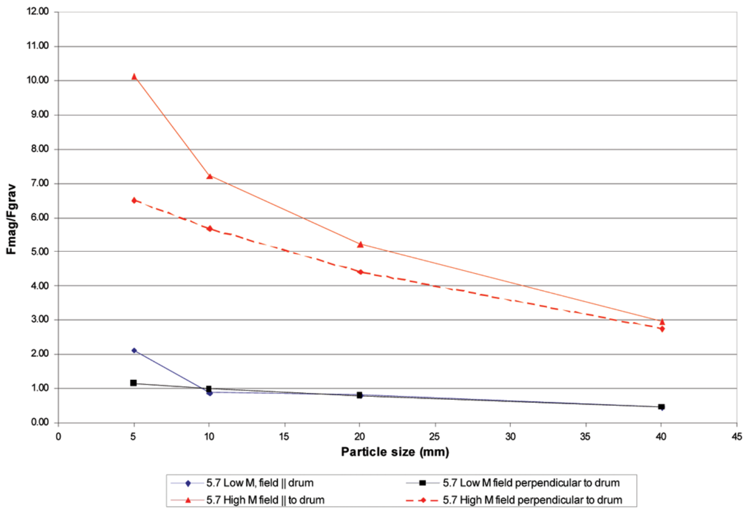

Figure 8—The ratio of magnetic to gravitational force for rocks of different size. The data have been calculated from the FEM models of a 400 mm drum

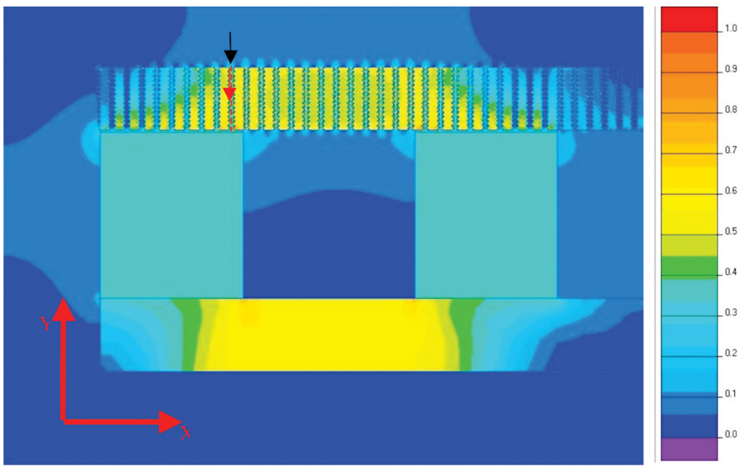

Figure 9—Magnetic flux density for one circuit of a WHIMS machine. The normalized magnetic flux density is shown on the right. The arrow indicates the location of a line contour for Figure 10

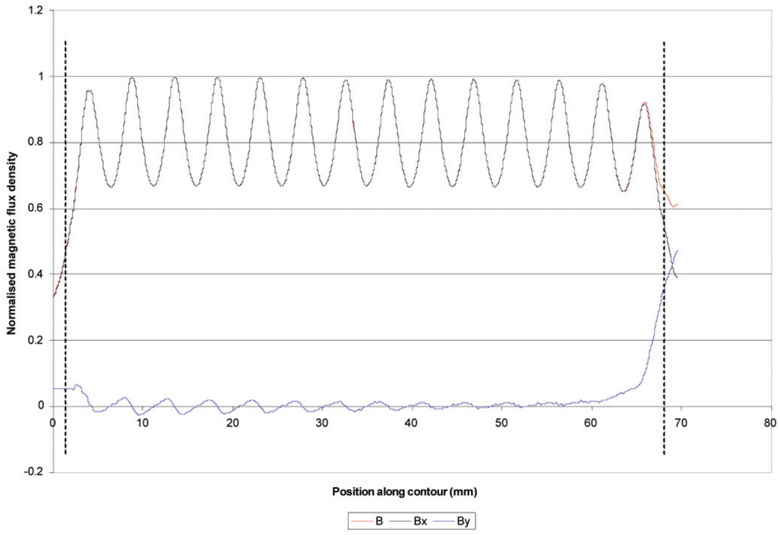

Figure 10—Normalized magnetic flux densities B, B_x and B_y for a contour drawn from the red arrow to the magnet equidistant between two salient plates as shown in Figure 9. The dotted lines indicate the beginning and end of the salient plate. B_x is the flux density component perpendicular to the salient plates and B_y is parallel to the salient plates

Key to the WHIMS design is the magnetic circuit and the achievable magnetic flux densities and magnetic field gradients. Figure 9 shows the results of FEM calculations from one such circuit in a WHIMS. It is clear from Figure 9 that the matrix is not always magnetically saturated, which has particular relevance to how and where the circuit should be fed with mineral slurry. Close examination of Figure 9 also shows significant colour (used to encode magnetic field strength) differences between the salient plate gaps and the salient plates themselves. These differences, as before, are indicative of the magnetic field gradients.

It is instructive to determine the magnetic field profile across the width of a salient plate gap. A contour was established at the arrow shown in Figure 9, the magnetic flux densities are shown in Figure 10. The dotted lines in Figure 10 show the limits of the width of the salient plate gap. As expected the normalized magnetic flux density varies periodically across the width in sympathy with the teeth of the salient plates. The transverse component of the magnetic field (B_y) is small indicating that the field gradients will also be small and cause very little movement of particles transverse to the slurry flow direction. However, the magnetic field B_x and field gradient in the x direction encourages magnetic particles to be attracted to and move towards the salient plate surfaces.

Electrostatic separation: results and discussion

The main prerequisite for electrostatic separation is that mineral particles acquire or have an electric charge. If a particle is charge neutral then the mechanisms for the separation of different mineral particles cannot occur in electrostatic separators.

The basic mechanisms by which particles may acquire a charge is by contact charging, which relies on different work functions on the surface of particles, induction charging which relies on the close proximity of charged surfaces or particles and corona charging. It is the latter which is principally considered in this paper since it is this method which is dominant in a high tension roll (HTR) separator and their modern equivalents. A schematic layout of a modern HTR type machine is shown in Figure 11.

When there is sufficient electric field near the small diameter corona wire, ions are produced due to electrons being removed from the surrounding gas molecules. If the electric field is large enough then the avalanche production of electrons is sustained. Corona charging of particles then occurs when charge carriers are swept onto the mineral particles by an electric field.

The key difference between the two possible polarities is how the avalanche electrons are created and the consequent electron densities in the plasma region. Up to a hundred times greater electron densities are possible with negative polarity. In both cases it is ionized gas molecules that are moved using the electric field between the corona wire and the earthed rotor. The ions are continually recombining with free electrons to provide neutral molecules again. Once this has occurred, these molecules have no further part to play in the electrostatic separator.

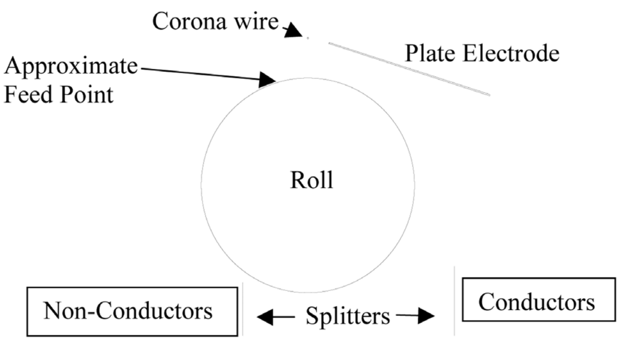

Figure 11—General layout of a roll type electrostatic separator. The roll rotates in a clockwise direction

The electric force (***F***) on a charge (*q*) due to an electric field (***E***) is described by Equation [4]. As before, bolded quantities represent vectors that have both magnitude and direction.

$$\mathbf{F} = q\mathbf{E} \qquad [4]$$

Since the mass of an ion is very small (≅10^{-25} kg) and the charge is also small (≅10^{-19} C) the electric force on an ion is of order 10^{-13} N with an electric field ≅10^{6} Vm^{-1}. Its acceleration is then of order 10^{12} ms^{-2}, so that a particle in the corona ion stream receives a significant amount of charge in a small amount of time if the ion production rate near the corona wire is also high. The ion production rate is related to the magnitude of the electric field at the corona wire which is determined by the spacing of the wire from the earthed rotor and the voltage applied to the corona wire.

Once charge is located on a mineral particle Equation [4] still applies but the mass of the particle is now of interest (≅10^{-10} kg) which together with a charge of order 10^{-6} C gives an electric force of approximately 1 N and an acceleration of ≅10^{10} ms^{-2}. These estimates mean that a charged particle should arrive at the rotor very quickly if it is airborne. The actual amount of charge that a particle can accept is dependent on the mineral and particle size.

Once a charged particle is located on or close to the metal roll, an opposite charge is established in the roll surface by electron movement (repulsion or attraction). Consequently, the particle is attracted to the roll surface very strongly. Traditionally the attraction force can be calculated by the method of images which allows the charge on the particle and the charge distribution in the roll to be treated as point charges so that Coulomb's law can be applied directly (Equation [5]). In Equation [5], q is the charge on the particle, ε_0 is a constant, R is the distance $\vec{R}$ between the particle and its image charge location, and is a unit vector between the charge and its image charge.

$$\mathbf{F} = \frac{1}{4\pi\varepsilon_0}\frac{q^2}{R^2}\vec{\mathbf{R}} \qquad [5]$$

The image force reduces quickly once the particle moves away from the surface; in fact it is only significant for particles that are within 2–3 diameters of the roll surface.

The force that a particle sees on the metal roll is the sum of all image forces including those from its neighbours. The image force on a particle calculated on its own is thus enhanced by the neighbouring imaging forces. There are also forces on a particle due to the direct interaction with the charges on its neighbouring particles. The size effects become even more important since a large particle could be expelled from the rotor surface prematurely.

When the charge on a particle has decreased sufficiently towards zero, by making contact with the roll surface, then it is a candidate for being removed from the roll by the centrifugal force on the roll rotating at an appropriate speed. Whether it does or not depends on the amount of charge on neighbouring particles and their physical proximity. In the case of a modern electrostatic machine, the plate electrode also plays a part in facilitating the removal of particles from a roll. Since the plate is at the same potential and polarity as the corona wire, particles need to reverse their charge polarity before being attracted to the plate electrode.

The previous (conventional) discussion assumes, amongst other things that the particle bed on the roll is rotating at the same speed as the roll. It does not take friction properly into account nor does it take into account all the details of the charge gain and loss. All of these processes influence the metallurgical separation of the mineral suites of interest and so it is worthwhile exploring the theoretical foundations of particle separations a bit further.

From the previous discussion, the key to the understanding of electrostatic separation using corona charging and roll machines is the electric field patterns that are generated between the electrodes and the earthed rotor. Finite element techniques can be used to determine these fields, by using established physical equations and self-consistency to describe the solution of a given electrode geometry. The results can then be used to determine particle trajectories and product stream characteristics.

Figure 12 shows the result of such calculations for a conventional high tension roll machine that consists of a corona wire and a 270 mm diameter metallic rotor only. The same rotor diameter has been used for Figures 13 and 14. A conventional earthed enclosure is used as the boundary of the problem. Since the conventional metallic support rod of the corona wire has not been included, the results are more indicative of the full pin configuration. The normalized electric field scale is shown on the right of Figure 12. Since the electric field is a vector quantity, it is important to view the x and the y components of the electric field separately.

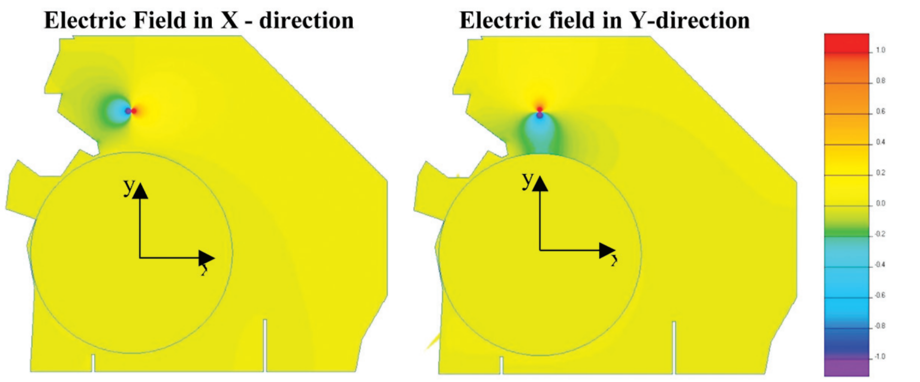

Figure 12—Electric fields in the X and Y direction for a conventional high tension roll machine without a plate electrode. The axes are also shown

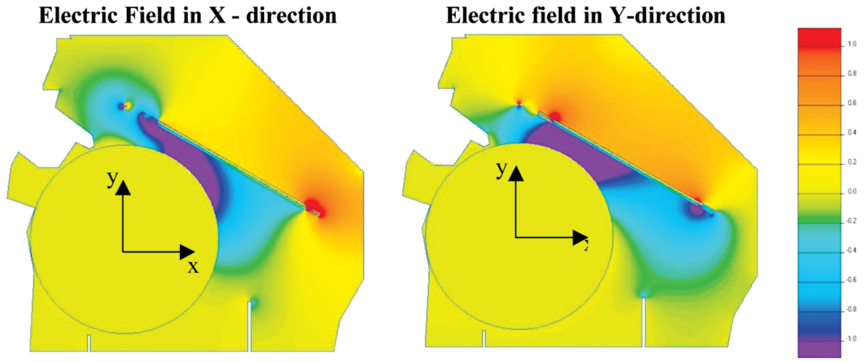

Figure 13—Electric fields in the X and Y direction for a high tension roll machine with a plate electrode. The plate electrode is uniform along its length

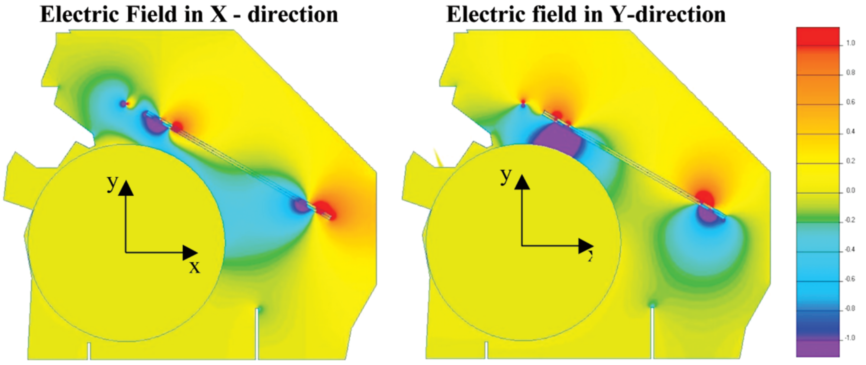

Figure 14—Electric fields in the X and Y direction for a high tension roll machine. The plate electrode is energized approximately 20 mm from each end

From the electric field plots of Figure 12 it is clearly evident that there is no or minimal electric field virtually everywhere for this configuration except close to the corona wire, located at top dead centre (TDC) above the roll. Due to the proximity of the earthed enclosure and roll there is an asymmetry in the electric field patterns for both the x and y components. This situation results in a significant number of the ions generated by the corona processes being ineffectual in charging the mineral particles because they do not reach them. Also, some of the ions that do move towards the particles on the roll recombine with electrons to form neutral molecules again. The acceleration of the ions to charge the mineral particles is in the $-y$ direction since virtually no $-x$ component of the electric field exists.

Figure 13 shows the electric field patterns of an electrostatic separator with an additional continuous copper plate electrode after the corona wire. The normalized electric field scale is shown on the right of Figure 13. The pre-normalized values of the electric fields are identical for Figures 12, 13 and 14. Significant electric fields exist in a large portion of the machine compared to the conventional HTR machine shown in Figure 12, providing an opportunity to adjust the electric separation characteristics in this zone using the plate electrode.

The key features of Figure 13 include

- The strong electric fields directed towards the roll in both the x and y direction (purple coding)
- The significant extent of these strong electric fields at the roll surface, helping to keep charged particles in place on the roll
- These strong electric fields also encourage any airborne charged particles to either move towards or away from the roll, depending on the charge polarity
- The electric field now has similar magnitude x and y components in the region between the corona wire and the metal roll so that the charged ions will now move in a curved path towards the roll, hitting the mineral particles sooner than for the HTR case of Figure 12, thus improving particle charging characteristics
- Closest to the roll, however, there is no x component of the electric field underneath the corona wire.

Figure 14 also shows the electric field pattern of a machine that is the same as that of Figure 13, except in this case the plate electrode has conducting copper for the first 20 mm and the last 20 mm of the plate length. In between there is only glass. It is clear that in this case the electric field patterns have changed again. When compared to Figure 13, Figure 14 shows:

- There is a lesser extent of strong electric fields between the plate and the roll. The x component at approximately 30 degrees after TDC, in particular, has half the magnitude to that shown in Figure 13
- At angles after approximately 50 degrees after TDC, the y component almost vanishes, encouraging airborne charged particles to move upstream back onto the roll or towards the roll, depending on charge polarity`
- The region under the corona wire is similar for Figures 13 and 14.

Understanding heavy mineral separation duties using finite element analysis

All three configurations of electrostatic separator show unique electric field patterns features which when combined with particle inertial and charge characteristics can be used to interpret particle trajectories and hence the metallurgical performance of the separators.

Conclusions

In this paper the principles of both magnetic and electrostatic separation have been described with the help of finite element modelling of the respective field patterns, which are determined by the geometry of the active and passive components. The value of finite element calculations has been shown to provide much needed information that relates separator geometry to the subtleties of both the electric and magnetic field patterns. The metallurgical performance of either a magnetic or electrostatic separator is dependent upon the magnetic and electric field patterns via the trajectories of particles through these fields. The expected qualitative performance of magnetic and electrostatic separators, as interpreted from FEM calculations, is in agreement with experimental experience. Further work is being done to make this agreement quantitative.

The fundamental understanding of the interactions between the particles, the physics surrounding the forces involved in affecting a separation, the geometry of the separator, and the mineralogy of the ore will be used to further develop these separation technologies. Such advances may significantly and positively affect the viability of future mineral sands projects that utilize these separation techniques.

Acknowledgement

The management of Mineral Technologies is acknowledged for allowing the publication of this paper.

References

Cheung, Y.K and Yeo, M.F. A *Practical Introduction to Finite Element Method*, Pitman Publishing, Marshfield, MA, USA. 1979.

Farrell, B., 'Loughlin, N.O., Judkins, D., Slyth, P., Hart, S., McGuire, T., and Russell, R. The Douglas Project Strandline Systems, Wimmera Region, Western Victoria, *Proceedings of the International Heavy Minerals Conference*, 18–19 June 2001, Fremantle, Western Australia, 2001. pp. 19–27

Frankl, D.R. *Electromagnetic Theory,* Prentice Hall, Inc., Englewood Cliffs, New Jersey, USA. 1986. ◆